

International Conference on Space Optics—ICSO 2022

Dubrovnik, Croatia

3–7 October 2022

Edited by Kyriaki Minoglou, Nikos Karafolas, and Bruno Cugny,



MEImage – Results of the mechanical and thermal verification campaign



METimage – Results of the mechanical and thermal verification campaign

Francesca Cucciarrè*¹, Michael Jentsch¹, Robert Schweikle¹, Heiko Joos¹, Armin Hauser¹, Werner Felder¹, Felix Rebell²

¹Airbus Defense & Space GmbH, 88039 Friedrichshafen, Germany

²DLR, Königswinterer Straße 522-524, 53227 Bonn, Germany

ABSTRACT

METimage is a cross-purpose, medium resolution, multi-spectral optical imaging radiometer for meteorological applications onboard the MetOp-SG satellites. It is capable of measuring thermal radiance emitted by the Earth and solar backscattered radiation in 20 spectral bands from 443 to 13.345 nm.

The instrument engineering model has been successfully tested and delivered to MetOp-SG. On METimage level this model served for instrument mechanical, thermal and EMC verification, at MetOp-SG level it supports the entire satellite test campaign. The sub-systems of the instrument engineering model are flight-like (primary and secondary structures, cryo-coolers and thermal-mechanical hardware) or qualification models (mechanisms, electronics). The optical subsystems are structural models. The mechanical and thermal test campaign allowed for successful verification of the instrument thermal and mechanical architecture and design, and successful validation of the mathematical models.

We present the results of the instrument thermal and mechanical test campaign and of the mathematical models correlation activities towards instrument PFM.

Keywords: METimage, MetOp-SG, EPS-SG, VII, multi-spectral, radiometer, thermal testing, mechanical testing

1. INTRODUCTION

METimage serves the VIS/IR Imaging Mission (VII) of the EUMETSAT Polar System – Second Generation (EPS-SG). The instrument is a passive imaging spectro-radiometer, capable of measuring thermal radiance emitted by the Earth and solar backscattered radiation in 20 spectral bands from 443 to 13.345nm [1]. Continuous scanning orthogonal to the flight direction ensures daily global Earth coverage with an across track swath of ~2670 km, a constant spatial sampling angle across the swath, and a spatial resolution of 500 m at Nadir. The scanning principle also allows for regular views to calibration sources without interruption of the scientific observation and for covering the entire optical and electrical chain. METimage operates on-board the MetOp-SG satellite A in a Sun-synchronous polar orbit with average altitude of 830 km.

The METimage instrument consists of the following main elements on the satellite's Nadir panel:

- The METimage optical head (MOH) contains the entire optical chain from the entrance aperture up to the detector proximity interface electronics. Designed as a box-structure made from sandwich panels (CFRP facesheets/Aluminium core) and isostatically mounted onto the satellite structure by 6 pendulum-struts, it supports:
 - All METimage optical assemblies (scanner assembly, telescope assembly, derotator assembly, cryogenic subsystem, including detectors);
 - several secondary structures (MOH and Instrument Support Structure Radiator Assembly, Nadir Baffle, Aperture Stops, connector brackets);
 - two calibration units (solar calibration device and the thermal calibration device);
 - Harness, purging sub-system and electrical bonding assembly.

*francesca.cucciarrè@airbus.com

- The external electronics assembly (EEA), mounted onto the satellite structure via Titanium blades, is realized by a dedicated support structure with radiator assembly and carries the front end proximity electronics and the thermal acquisition electronics unit. It is located just next to the optical head to ensure short paths for the analogue signals.
- The solar calibration device baffle (SCBA), mounted onto the satellite structure via CFRP/Titanium struts, allows for minimizing the stray light coming to the detector during the solar calibration thanks to an aluminium black-coated baffling structure.
- MLI: wrapping the MOH, the EEA and the SCBA (with exception of the optical apertures, radiative surfaces and harness feed-through), it allows for limiting the radiative heat exchange with the external thermal environment.

The METimage central electronics, the cryo-cooler electronics and the cryo-cooler cross-strap box are accommodated inside the payload equipment bay on the satellite's anti-Nadir panel and are connected to the electronics units on the Nadir panel via the external harness.

The thermal and mechanical test campaign on METimage engineering model described hereafter focused on the Nadir panel units, as the payload equipment bay units have been tested at equipment level.

The instrument configuration for the Nadir panel units is shown in Figure 1.

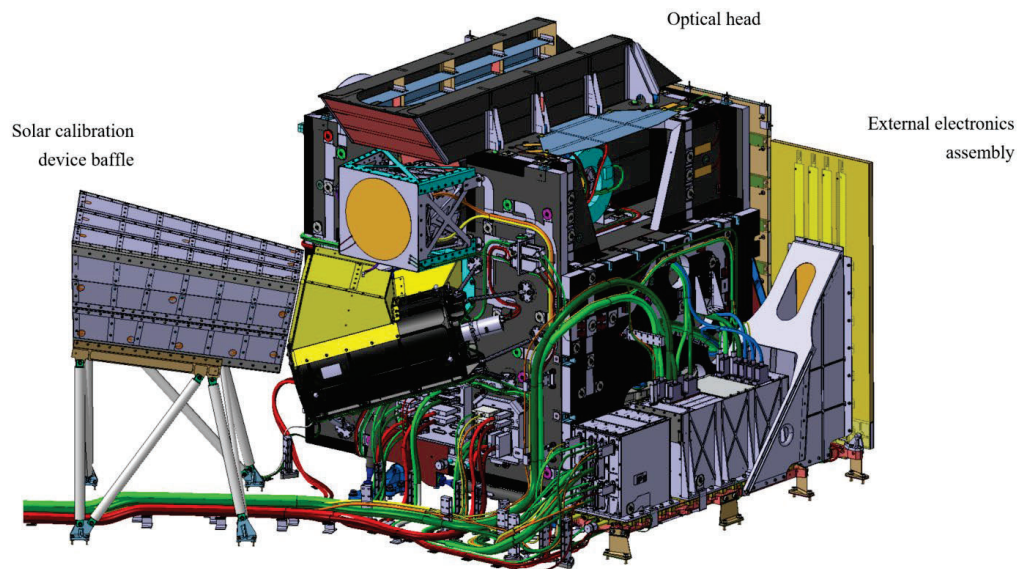


Figure 1. METimage Nadir panel sub-assemblies – MOH, EEA and SCBA (MLI not shown).

Figure 2 and Figure 3 provide some insight on the main sub-systems of the Nadir panel Units – MOH, EEA and SCBA.

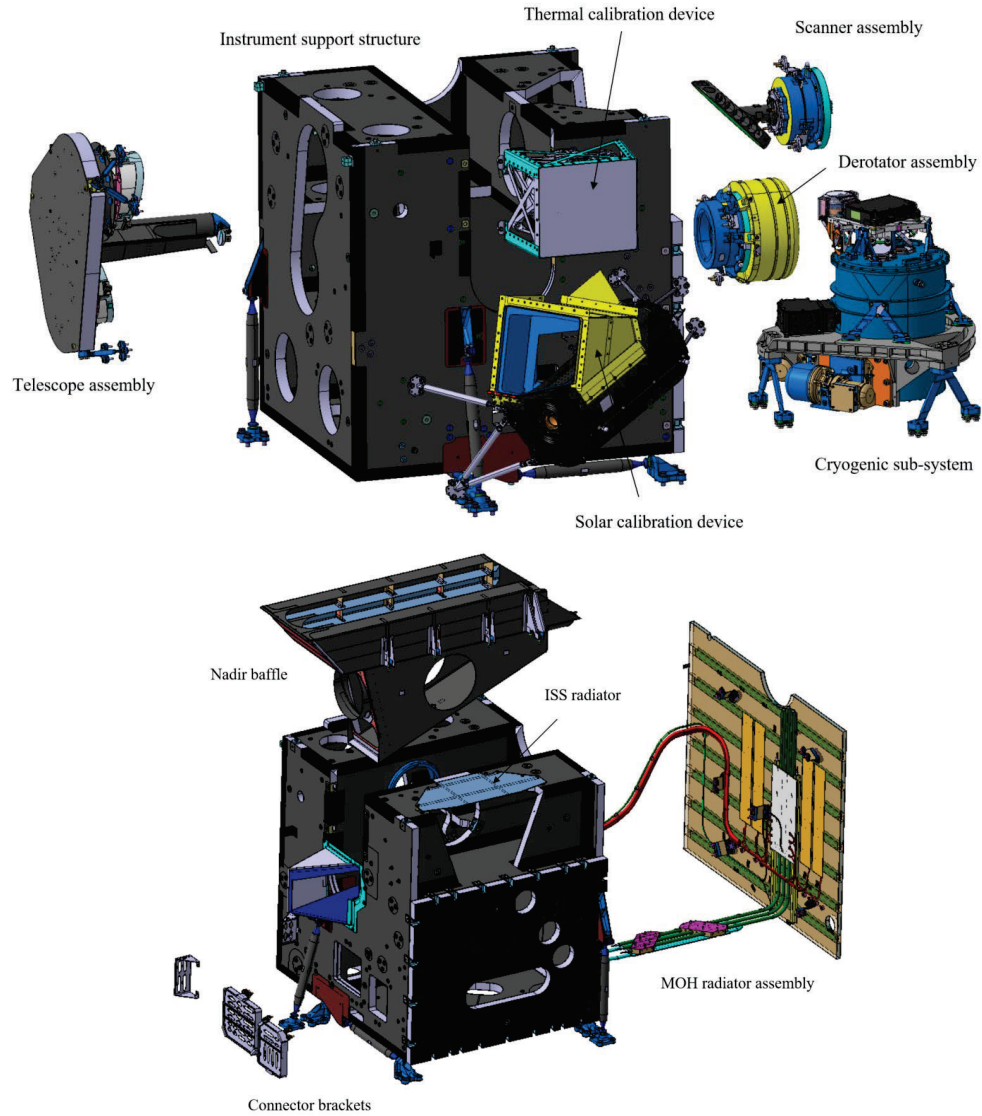


Figure 2. Main sub-assemblies of the Nadir panel units: MOH exploded view.

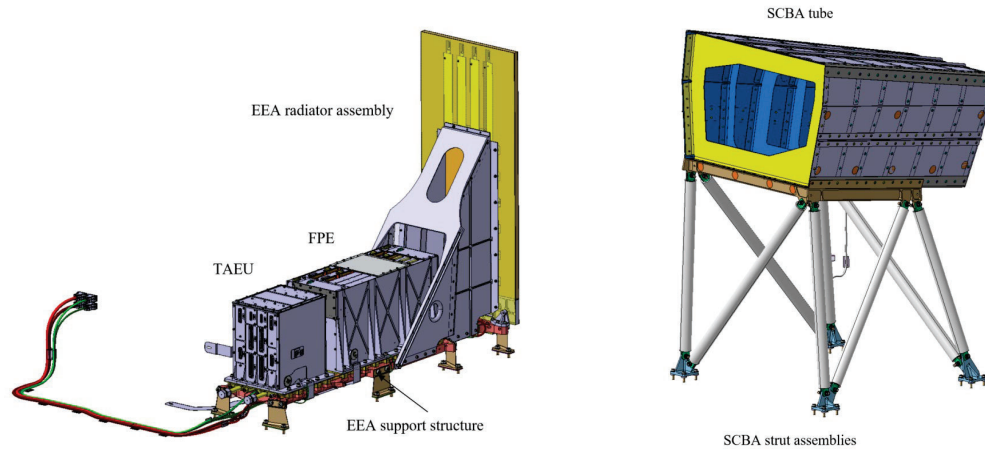


Figure 3. Main sub-assemblies of the Nadir panel units: external electronics assembly (left) and SCBA (right).

For the instrument development, a proto-flight approach is applied, supported by development models and breadboards on subsystem and equipment level, as technical and schedule risk mitigation.

2. INSTRUMENT ENGINEERING MODEL

The instrument engineering model is fully representative of the instrument PFM, with exception of the optical elements; all thermal, mechanical, electrical and functional interfaces to the satellite are flight representative.

The engineering model allowed for early mechanical, thermal and EMC verification and, after successful completion of the environmental testing at instrument level, has been delivered to MetOp-SG to support the execution of the satellite PFM test campaign; after completion of the satellite test campaign, it will be dismantled and replaced by the METimage PFM.

As shown in Table 1, which describes the as-built configuration, the sub-systems of the instrument engineering model are flight-like (primary and secondary structures, cryo-coolers and thermal-mechanical hardware) or qualification models (mechanisms, electronics); the optical subsystems are structural models.

Table 1. METimage engineering model as-built standard.

Sub-system	Build Standard
Instrument Support Structure (ISS)	Flight model
MOH Radiator Assembly	Flight model
Nadir Baffle Assembly (NBA)	Flight model
ISS Radiator	Flight model
Solar Calibration Device (SCAD)	Qualification model
Thermal CALibration Device Blackbody (TCAD)	Structural thermal model; no optical coatings
Scanner Assembly	Qualification model; no optics, mirror replaced by mass dummy
Derotator Assembly	Qualification model, with mirror mass dummy
Telescope Assembly (TELA)	Structural model: Telescope Structure flight model and mirrors structural thermal models
Entrance Stop Assembly	Structural model
SCAD Stop Assembly	Mass dummy
Cryogenic Subsystem (CGSS)	STM+; no optics, EM detectors
Cryo Cooler Electronics (CCE)	Nominal & redundant CCE, flight models
Cross Strap Box (XSB)	Qualification model

Sub-system	Build Standard
External Electronics Assembly (EEA)	Structure flight model; FPE qualification model; TAEU flight model
METimage Central Electronics (MCE)	Engineering model, only Nominal side present
Harness	Combination of test and flight harness
SCAD Baffle (SCBA)	Structural thermal model

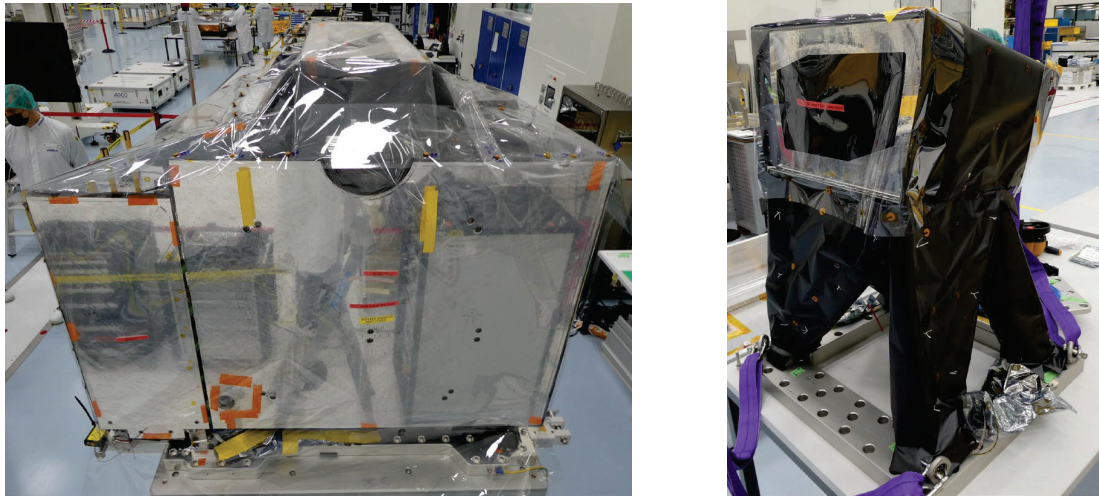


Figure 4. Optical head and external electronics assembly (left) and solar calibration device baffle (right).

3. THERMAL AND MECHANICAL TEST FLOW ON METIMAGE ENGINEERING MODEL

The thermal and mechanical test campaign with the METimage engineering model has taken place at Airbus Defense & Space GmbH premises in Friedrichshafen and EVT SAS premises in Toulouse from September 2020 until May 2021. A proto-flight verification approach has been applied, in order to avoid over testing, since several sub-assemblies and sub-systems of the engineering model will be refurbished and re-used on the METimage third flight model.

The solar calibration device structural thermal model (SCBA), which is part of the engineering model, has been included in the mechanical test configuration only prior acoustic testing, since a dedicated mechanical and thermal test campaign had taken place at Airbus Defense & Space GmbH premises in Friedrichshafen in the frame of the METimage STM campaign in 2018.

Here below the mechanical and thermal test flow is shown.

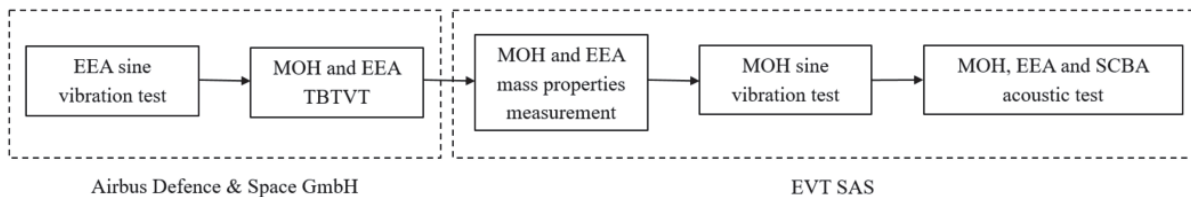


Figure 5. Mechanical and thermal test flow for the engineering model.

4. EXTERNAL ELECTRONICS ASSEMBLY SINE VIBRATION TEST

The EEA sine vibration test has been performed between September 17th and 18th 2020 in the vibration test facility at Airbus Defence and Space GmbH in Friedrichshafen.

The main test objective was to perform qualification under quasi-static and sine environmental loads according to project specification of the flight structures belonging to the EEA (main structure assembly and radiator assembly). In addition, thanks to correlation between analysis and test results, the validation of the finite element models was possible.

The tables below report the test levels.

Table 2. EEA quasi-static qualification levels.

Quasi static load	In plane [g]	In plane [g]	Out of plane [g]
	X_{EEA}	Y_{EEA}	Z_{EEA}
Applied separately	±12.5		
Applied separately		±8.8	
Applied separately			±8.8
Combined loading	±7.5	±5.0	
Combined loading	±7.5		±5.0
Combined loading		±5.0	±5.0
Combined loading	±9.0		±4.0

Table 3. EEA sine vibration qualification levels.

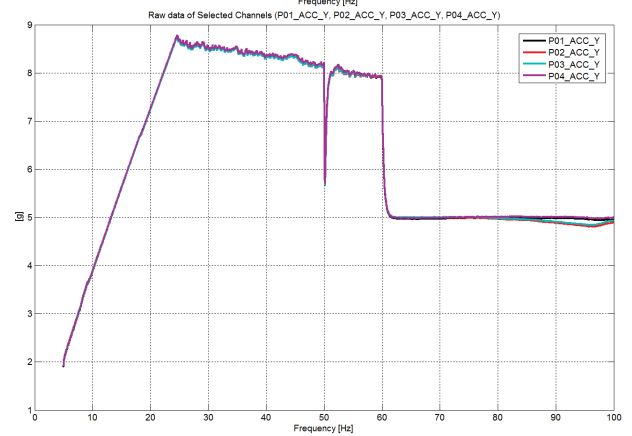
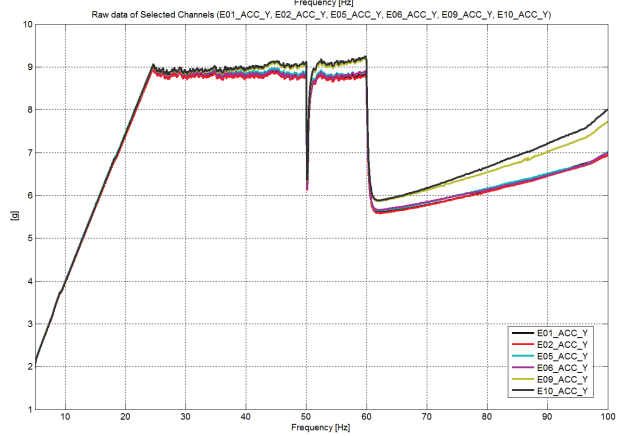
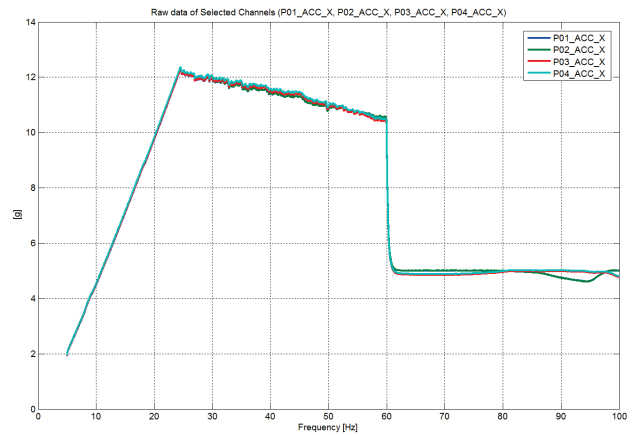
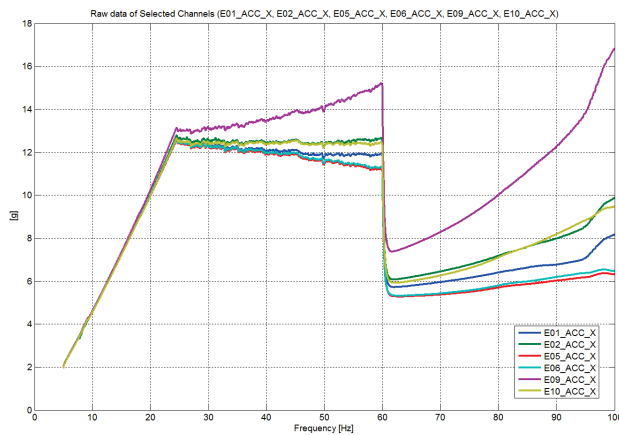
In plane [g]	In plane [g]	Out of plane [g]
X_{EEA}	Y_{EEA}	Z_{EEA}
5 to 25 Hz – 2 to 12.5g	5 to 25 Hz – 2 to 8.8g	5 to 25 Hz – 2 to 8.8g
25 to 60 Hz – 12.5g	25 to 60 Hz – 8.8g	25 to 60 Hz – 8.8g
60 to 100 Hz – 5g	60 to 100 Hz – 5g	60 to 100 Hz – 5g

The figure below shows the EEA engineering model under test on the shaker: in total four pilots and co-pilots were used for controlling the input and 13 accelerometers for monitoring.



Figure 6. EEA engineering model – including MLI – on the shaker.

The plots below show the reached levels on qualification load and the pilot responses for the three different axes.



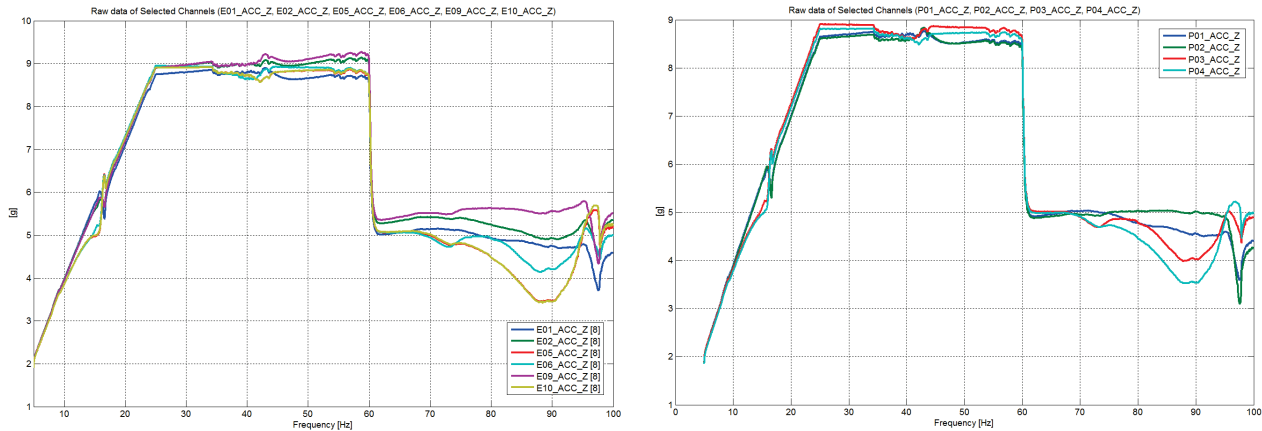


Figure 7. Reached levels on qualification load and pilot responses for the axes X (top), Y (middle), Z (bottom).

The decrease of the input acceleration along the Y axis at 50Hz has been connected to an issue of the shaker control system, however this did not invalidate the results of the test, since the decrease was limited to less than 1 second. Along Z, the mode of the head expander and the shaker introduced some control issues above 80Hz, however not considered critical for the purpose of the test.

The hardware passed the qualification test under acceptance duration without any degradation or damage, as proven by the detailed inspections and resonance search after every run; in addition, the dynamic behaviour of the structure was according to the predictions: no detailed finite element model correlation was needed.

5. METIMAGE OPTICAL HEAD SINE VIBRATION TEST

The MOH sine vibration test has been performed between April 27th and May 7th 2021 in the vibration test facility at EVT SAS in Toulouse.

The main test objective was to perform qualification under quasi-static and sine environmental loads according to project specification of the MOH, including primary and secondary structures. In addition, thanks to correlation between analysis and test results, the validation of the finite element models was possible.

The tables below report the test levels.

Table 4. MOH quasi-static qualification levels.

Quasi static load	In plane [g]		Out of plane [g]
	X _{MOH}	Y _{MOH}	Z _{MOH}
Applied separately	±12.5		
Applied separately		±8.8	
Applied separately			±8.8
Combined loading	±7.5	±5.0	
Combined loading	±7.5		±5.0
Combined loading		±5.0	±5.0
Combined loading	±9.0		±4.0

Table 5. MOH sine vibration qualification levels.

In plane [g]	In plane [g]	Out of plane [g]
X_{MOH}	Y_{MOH}	Z_{MOH}
5 to 25 Hz – 2 to 12.5g	5 to 25 Hz – 2 to 8.8g	5 to 25 Hz – 2 to 8.8g
25 to 60 Hz – 12.5g	25 to 60 Hz – 8.8g	25 to 60 Hz – 8.8g
60 to 100 Hz – 5g	60 to 100 Hz – 5g	60 to 100 Hz – 5g

The figure below shows the MOH engineering model under test on the shaker, wrapped within the contamination protection cover: in total four pilots and co-pilots were used for controlling the input and 66 sensors (accelerometers, strain gauges and sensors) for monitoring.

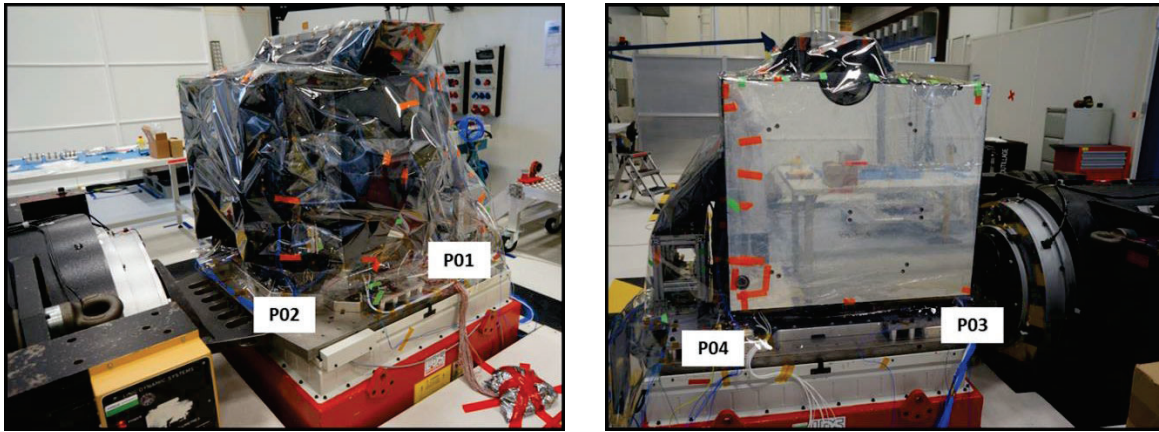


Figure 8. MOH engineering model – including MLI and contamination protection cover – on the shaker.

Before test, the notching strategy had been agreed with the satellite technical authorities: the main drivers for the definition of the notching philosophy were given by the limit loads of the struts connecting the main structure inserts to the satellite interface, as reported in the table below.

Table 6. MOH struts limit loads not to be exceeded during MOH qualification sine vibration test.

Strut	Limit load [kN]
1	15.6
2	16.8
3	16.4
4	15.6
5	15.6
6	15.6

The plots below show the input profiles, the manual notch profiles and the levels reached by the channels, which triggered the notching along the three axes; also, the frequency ranges affected by the notching are shown below.

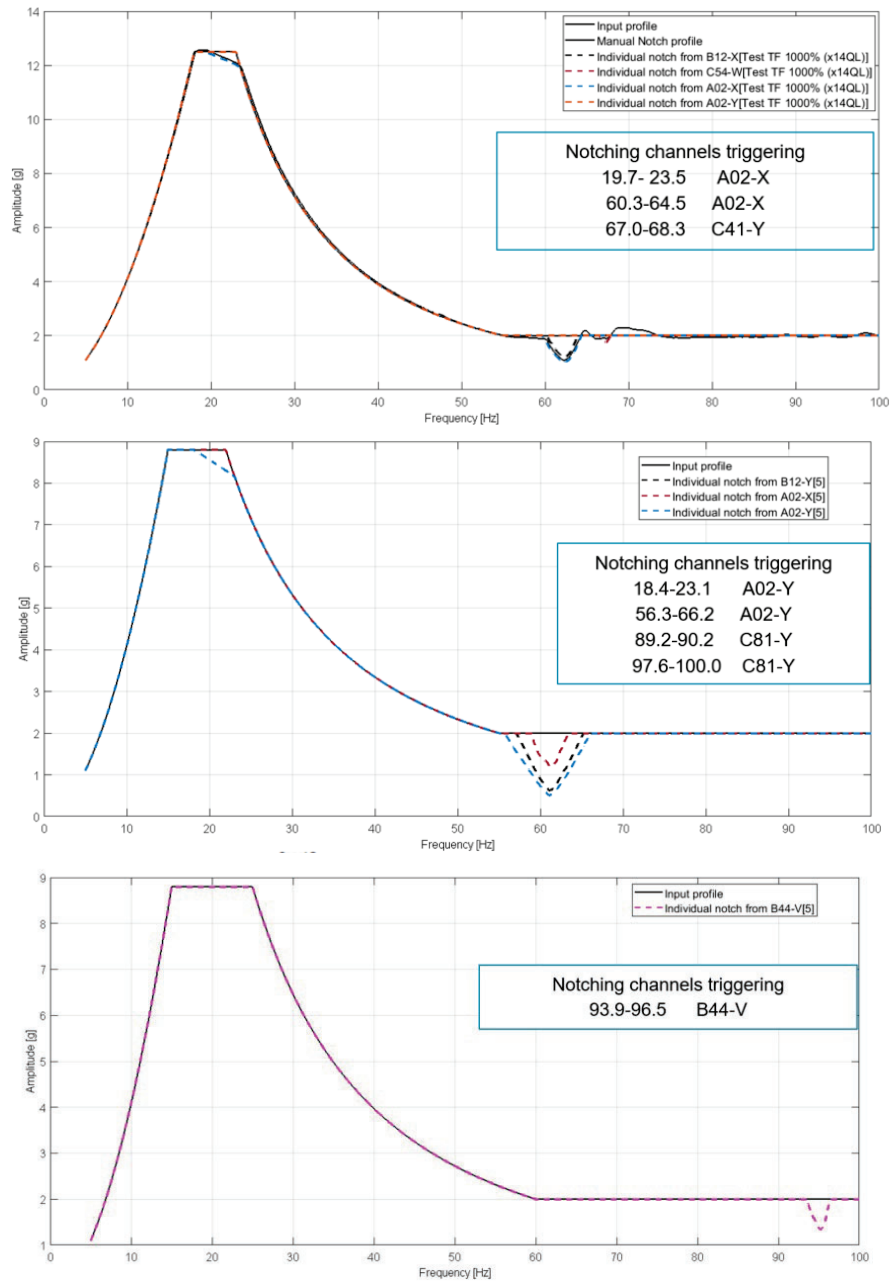


Figure 9. Input profiles, manual notch profiles and the levels reached by the notching channels for the axes X (top), Y (middle) and Z (bottom).

The hardware passed the qualification test under acceptance duration without any degradation or damage, as proven by the detailed inspections and resonance search after every run.

As an example, some pre-post signature comparison plots are reported in the following pictures.

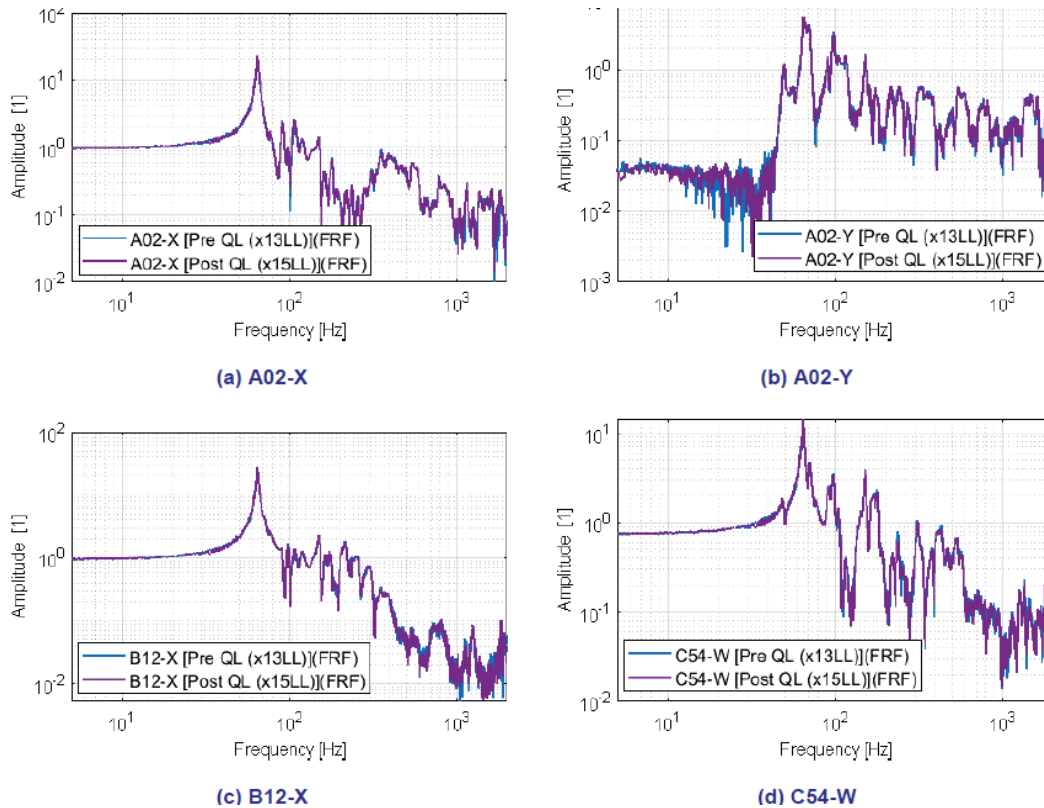


Figure 10. Pre- and post- signatures comparisons for some channels along different axes.

The finite element model of the MOH has been correlated by comparison of the test results and test predictions. The following parameters have been adapted:

- the mass and the mass distribution of the object under test, which had been measured before the sine vibration test;
- stiffness of the main structure to the strut assemblies;
- stiffness of the strut assemblies;
- stiffness of bolted joint connection between strut assemblies and test adapter;
- stiffness of the bolted joint connections within the test adapter itself.

The following table shows a comparison between the mass and centre of gravity as assumed in the predictions and the measured mass and centre of gravity.

Table 7. Mass and centre of gravity coordinates as considered in the test predictions and measured values.

	Mass [kg]	Centre of gravity [mm]		
		X	Y	Z
Predicted	189.9	606.7	-491.2	463.2
Measured	175.8	606.9	-489.9	462.1

The following table shows how adapting mass, mass distribution and stiffness at the main interfaces allowed for validation of the finite element model for the in-plane modes.

Table 8. Impact of mass and stiffness parameters adaptations on the calculated in-plane eigenmodes.

Configuration	Mass [kg]	Frequency 1 [Hz]	Frequency 2 [Hz]
Test predictions	189.9	64.9	67.1
Test results	175.8	61.1	62.7
Adaptation of mass and mass distribution	175.8	66.6	68.6
Adaptation of mass and I/F stiffness	175.8	61.2 (Y)	64.8 (X)

Detailed investigations in the frame of the model correlation, considering the test results on the Z axis and the MAC values, clearly revealed a coupling between the MOH and the shaker system. The out-of-plane main mode at 88-89Hz could be identified as cross mode for in-plane excitation; for out-of-plane excitation in Z, none of the predicted modes could be really excited and properly compared.

6. METIMAGE ACOUSTIC TEST

The METImage acoustic test has been performed between May 11th and May 12th in the acoustic chamber at EVT SAS in Toulouse.

The main test objective was to perform qualification of the engineering model, including its sub-systems, under acoustic environmental loads according to project specification, demonstrating at the same time the strength was high enough to environmental conditions during testing.

Table 9. Qualification acoustic loads.

Frequency [Hz]	Acoustic qualification load [dB]
31.5	135
63	138.5
125	141
250	141.5
500	137
1000	129
2000	123
4000	119
OASPL	146.3

The figure below shows the engineering model - wrapped within the contamination protection cover - in the reverberant chamber; in total 9 microphones were placed in the chamber and 94 sensors (accelerometers, strain gauges and sensors) were installed for monitoring on the hardware under test.

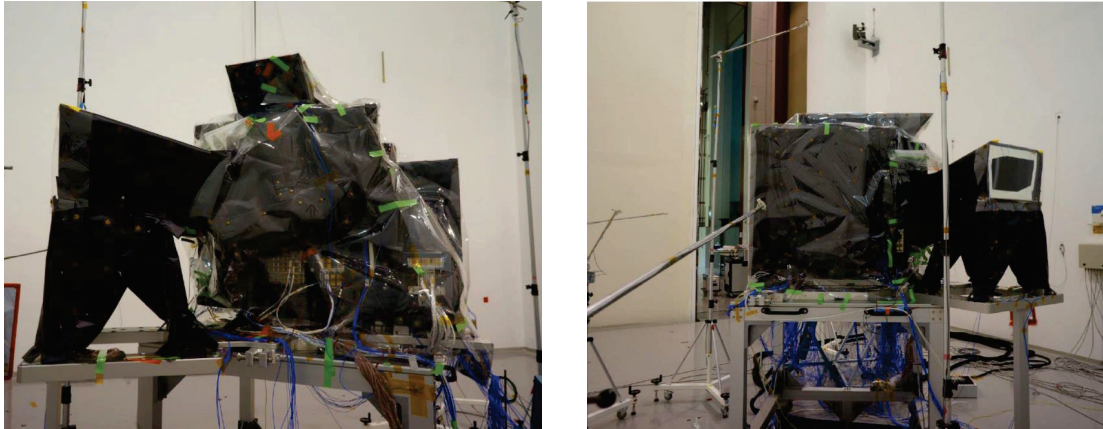


Figure 11. Engineering model (MOH, EEA and SCBA) in the acoustic chamber.

The acoustic test allowed for checking the margins with respect to the random environment requirements specified at the sub-assemblies interfaces: all measured accelerations at the sub-assemblies interfaces were lower than predicted.

The hardware passed the qualification test under acceptance duration without any degradation or damage, as proven by the detailed inspections and resonance search after every run.

As an example, a pre-post signature comparison plot is shown in the following picture.

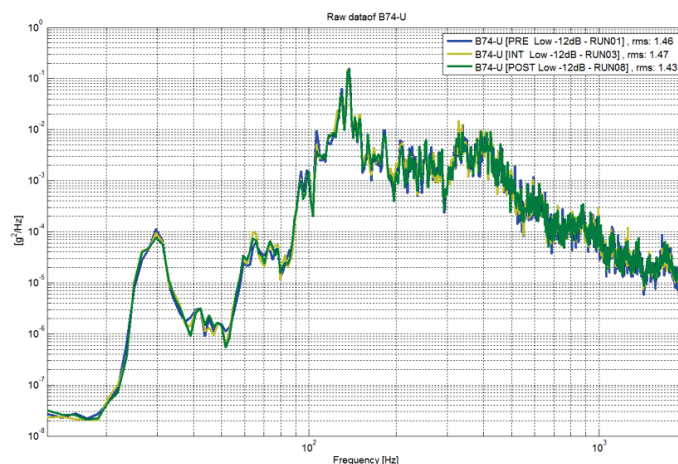


Figure 12. Pre- and post- signatures comparison for the Nadir baffle accelerometer in X direction.

7. THERMAL TEST CAMPAIGN

The thermal vacuum (TV) and thermal balance (TB) test campaign has been performed in the thermal vacuum test facility of Airbus Defence and Space GmbH in Friedrichshafen from March 8th to March 29th in 2021.

The main objectives of the test are listed here after:

- Bake-out of the METimage engineering model at 50°C +5K including TQCM.
- Verify proper function of the nominal and redundant thermostat controlled survival heater circuits.
- Demonstrate compatibility of the design within the specified non-operational design temperature range in vacuum.
- Verify decontamination requirements during warm-up from survival to operational conditions.

- Provision of test data (temperature distribution and electrical power dissipation of heaters, mechanisms, cryocoolers, electronics boxes) for correlation of the thermal mathematical models.
- Quantify the resulting temperature gradients within the CFRP panels during thermal balance phases as input for structural thermal optical and performance analyses.
- Perform micro-vibration measurement to characterize the micro-vibration sources acting within the instrument (mechanisms, including cryocooler).
- Perform reduced functional test at ambient conditions and full functional test in vacuum at several temperature levels (hot and cold).

The test configuration with the MOH and the EEA - including MLI, test and flight harness - within the chamber is shown in the following pictures.

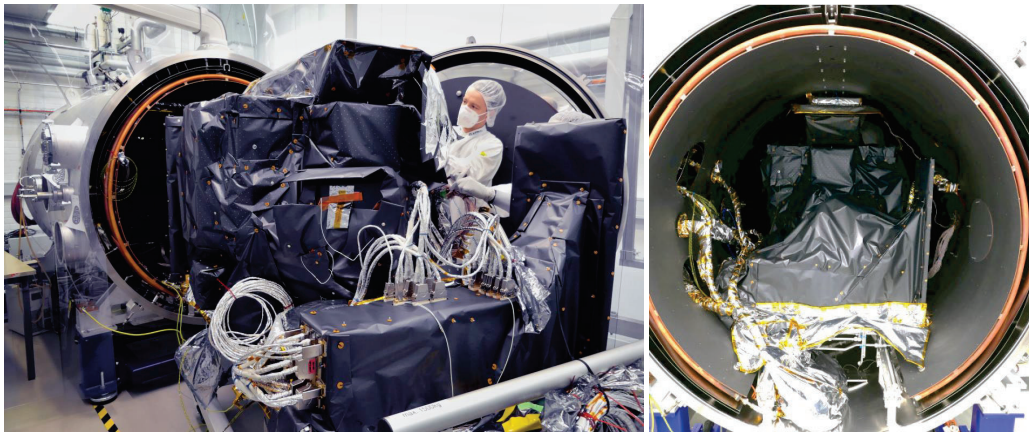


Figure 13. MOH and EEA engineering models during integration activities (left) and prior chamber closing (right).

The graph hereafter depicts qualitatively the different test phases:

- Initial bake-out phase at hot non-operational temperature;
- Nominal survival phase, for verification of the nominal survival heaters and thermostats;
- Redundant survival phase, for verification of the redundant survival heaters and thermostats;
- Phase at cold non-operational temperature;
- Decontamination phase;
- Cold and hot thermal balance phases, including micro-vibration measurement of the micro-vibration sources (mechanisms, including cryocoolers), thanks to 5 micro-vibration sensors and 6 strain sensors, and full functional tests;
- Recovery to ambient.

Two reduced functional tests at ambient – before and after thermal vacuum test – have been performed as well.

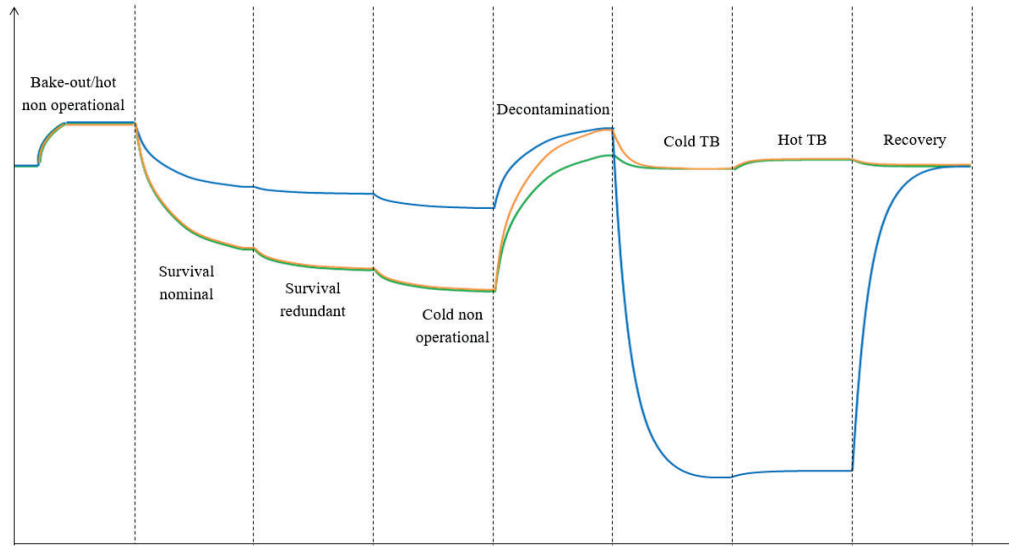


Figure 14. Thermal vacuum (TV) and thermal balance (TB) test profile.

The hot and cold non-operational phases and two thermal balance phases have been conducted as planned and the engineering model thermal vacuum and thermal balance test has been performed successfully.

Proper functionality of the thermostats has been verified both for the nominal and redundant survival heater chains; in addition, the minimum non-operational temperature targets for the primary and secondary structures could be fully reached on several parts of the hardware, with exception of very minor deviations due to the as-built configuration. The warm-up to operational conditions using the nominal decontamination and operational heater circuits has been performed, followed by the cool-down phase of within the cryostat by operating the TMUs until achievement of cryogenic conditions on the infrared detectors, which have been successfully operated at 58.5K. The functionality of instrument radiators, including the heat pipes chain, has been and shown.

During two thermal balance phases, the stability criteria have been reached for all temperature sensors and thus provided a reliable input for the thermal mathematical model correlation.

During the test, up to 16 microvibration measurements were sequentially conducted. The evaluation of the I/F forces led to the conclusion that, when operating the microvibration sources, the response levels in all 3 directions were in the same order of magnitude as the noise level at low frequencies. In addition, the comparison between predictions and test results for the operational scenario showed that the measured levels above 50Hz were in the same order of magnitude of the predictions.

Thanks to the successful bake-out, the risk of contamination on the instrument during later test stages and for the satellite platform and other instruments during the thermal vacuum test on satellite level has been minimized.

Some results of the thermal balance and thermal vacuum test campaign are shown hereafter.

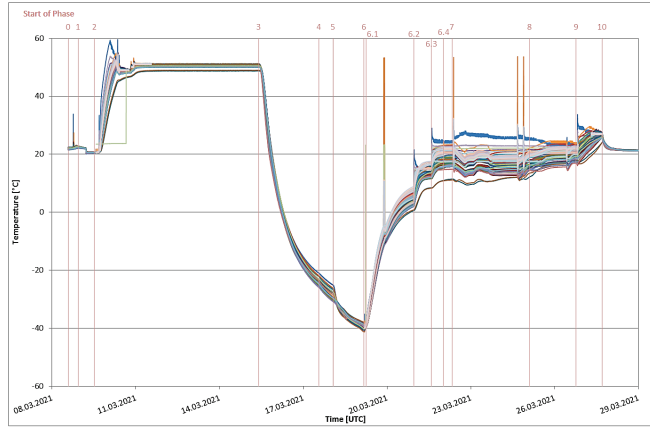


Figure 15. Temperature profile on the instrument support structure during test.

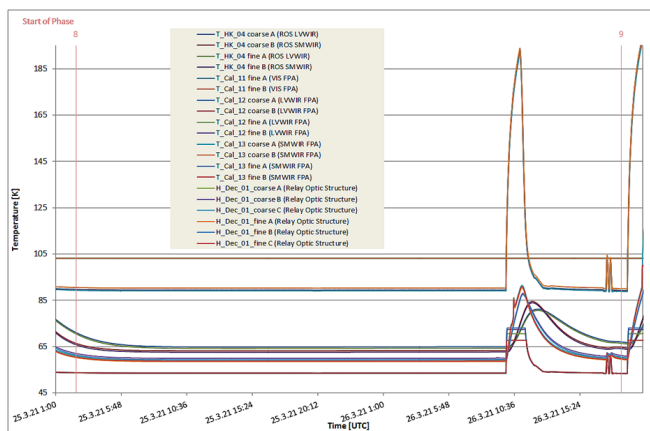


Figure 16. Temperature profile on the cryogenic sub-system during test.

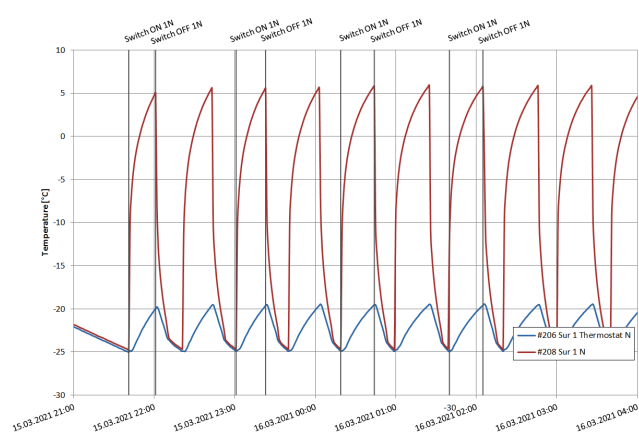


Figure 17. Nominal survival heater 1 switch-on and -off cycle.

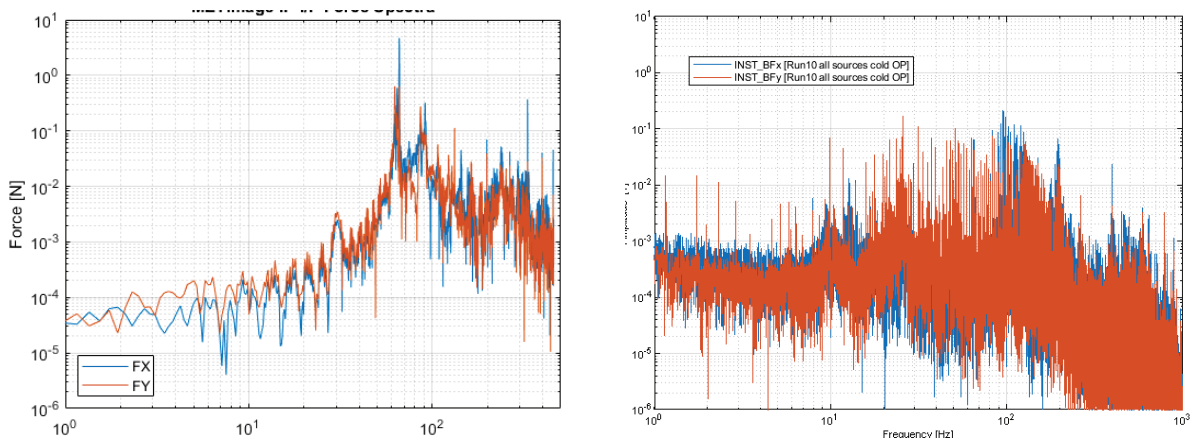


Figure 18. Comparison of in-plane base forces [N] from analysis (left) and test results (right).

The data acquired during the thermal balance phases allowed for extensive correlation of the geometrical and thermal mathematical models. Prior correlation, several adjustments have been considered in order to adapt the thermal model used for the predictions to the as-built standard of the engineering model. Hereafter some adaptations are listed:

- Shrouds temperatures adapted to measured temperatures during TB Phases.
- Position of the test object has been adapted within the chamber.
- MLI surrounding the instrument support structure radiator area has been adapted to as built status.
- Thermo-optical properties of some components has been adjusted to reflect the as-built status.
- The dissipation values of the scanner and derotator mechanisms and electronics boxes have been adapted to the values measured during test.

In the frame of the correlation, in addition, several internal conductive couplings have been modified, the cryocoolers performance has been slightly increased for low cooler input power values and the MLI integration factor has been adjusted for several blankets.

As a result of the model correlation, the temperature deviations between the thermal model and the measured test results could be reduced significantly, with a maximum temperature deviation of approximately 4K for the cooler flight thermistor and a maximum duty cycle deviation of 30% for the EEA.

ACKNOWLEDGEMENTS

The work described was performed on behalf of the German Space Administration with funds from the German Federal Ministry of Transport and Digital Infrastructure and co-funded by EUMETSAT under DLR Contract No. 50EW1521.

REFERENCES

- [1] O. Wallner, K. Ergenzinger, R. Rivière, F. Schmülling, “METimage – PFM Status Report”, these proceedings